THE JOURNAL OF CHEMICAL PHYSICS **131**, 124118 (2009)

Response properties with explicitly correlated coupled-cluster methods using a Slater-type correlation factor and cusp conditions

Matthias Hanauer[a] and Andreas Köhn[b]
Institut für Physikalische Chemie, Universität Mainz, D-55099 Mainz, Germany

(Received 22 July 2009; accepted 7 September 2009; published online 29 September 2009)

The recently proposed extension of the explicitly correlated coupled-cluster ansatz using cusp conditions [A. Köhn, J. Chem. Phys. **130**, 104104 (2009)] is tested for suitability in the calculation of response properties. For this purpose, static and dynamic electrical properties up to ESHG hyperpolarizabilities as well as optical rotations have been computed within the CCSD(F12) model. It is shown that effectively converged correlation contributions can reliably be obtained using augmented quadruple zeta basis sets already. The ansatz is optionally equipped with an extension capable of reducing the one-electron basis set error. A further simplification of the method specific Lagrangian aimed at reducing the computational effort has been tested and is shown to be uncritical. Furthermore, we examined the impact of conventional triple and quadruple excitations in explicitly correlated property calculations. © *2009 American Institute of Physics*. [doi:10.1063/1.3238237]

I. INTRODUCTION

Response theory describes the impact of a generally time-dependent perturbation on an atom or molecule.[1,2] Applied to coupled-cluster (CC) methods[3] it is a powerful tool for the accurate calculation of atomic and molecular properties. However, highly accurate coupled-cluster computations are limited to very small systems due to a slow basis set convergence of correlation contributions. R12 and F12 methods deal with that problem by making explicit use of the interelectronic distance r_{12} in form of a correlation factor in the ansatz for the wave function.[4–6] Additional three- and four-electron integrals are avoided by suitable approximations including resolution of the identity approximations.[7,8] In the original R12 methods, explicitly correlated functions are generated by action of the correlation factor on the reference determinant. These functions suffice for an enhanced description of the ground state and could even be successfully used to accelerate the basis set convergence of several electrical properties[9] and structural parameters as well as harmonic frequencies for excited states.[10] However, it has been shown that a proper description of excited electronic states requires the use of additional functions generated by action of the correlation factor on excited determinants.[11] For that purpose, Neiss *et al.* proposed to add a small number of excited determinants within the CCSD(R12) model, selected on the basis of seminatural MP2 occupation numbers.[12] Recently, one of the present authors[13] suggested a more general ansatz that employs all available singly excited determinants while using a Slater-type correlation factor $f(r_{12}) \sim e^{-\gamma r_{12}}$ within the CCSD(F12) model.[14,15] It is based on Ten-no's SP approach[16] which can be derived from the F12 ansatz by fixing the F12 coefficients in a way that ensures the fulfillment of the *s*- and *p*-wave cusp conditions,[17] and has therefore been termed extended SP (XSP) approach. As the XSP ansatz has been shown to substantially improve the basis set convergence of the correlation energy of excited states, it can be expected to perform well when applied to the calculation of other response properties. To demonstrate this is the purpose of the present work. In addition to the approaches SP and XSP, an extension aimed at improving the convergence of the one-electron contributions will be discussed. Furthermore, less time-consuming modifications of the employed F12 methods are tested, in which most of the additional terms arising from the so-called ansatz 2 are omitted, analogous to modifications proposed by Werner and co-workers.[18,19]

II. THEORY

A. Explicitly correlated coupled-cluster methods

In coupled-cluster theory, geminals can be included in the ansatz for the wave function,

$$|\Psi\rangle = e^{S}|0\rangle, \tag{1}$$

by augmenting the conventional cluster operator with an additional operator T' that generates explicitly correlated functions from the reference state $|0\rangle$:

$$S = T + T'. \tag{2}$$

In spin-orbital formalism, the conventional cluster operator is defined as

$$T = \sum_{i=1}^{N} T_i = T_1 + T_2 + \cdots = t_a^i a_i^a + \frac{1}{4} t_{ab}^{ij} a_{ij}^{ab} + \cdots , \tag{3}$$

with $N=1,2,3,4$ for CCS, CCSD, CCSDT, and CCSDTQ, respectively. $a_{pq}^{rs} = a^r a^s a_q a_p$ denotes a string of creation operators a^r and annihilation operators a_p, and we make use of the Einstein sum convention. For index conventions, see Table I.

Within Ten-no's SP approach,[16] the operator

---

[a] Electronic mail: hanauem@uni-mainz.de.

[b] Electronic mail: andreas.koehn@uni-mainz.de.

$$T'_{\mathrm{SP}} = \mathcal{R} = \tfrac{1}{4}\mathcal{R}^{ij}_{\alpha\beta}a^{\alpha\beta}_{ij} \tag{4}$$

incorporates the action of a correlation factor $f(r_{12}) \sim r_{12} + O(r_{12}^2)$ on the reference determinant through excitations into a formally complete virtual orbital space. $\mathcal{R}^{pq}_{\alpha\beta}$ is defined in Table I and constitutes an integral over the correlation factor, scaled and symmetrized in a way that fulfills the *s*- and *p*-wave cusp conditions.[13,20]

The XSP approach, described in Ref. 13, additionally employs geminals generated from the action of $f(r_{12})$ on singly excited determinants, which are crucial for a proper description of the response of a molecule to external fields. This is done by including the operator

$$[\mathcal{R},\tilde{T}_1] = \tfrac{1}{2}\mathcal{R}^{ia}_{\alpha\beta}\tilde{t}^{j}_{a}a^{\alpha\beta}_{ij}. \tag{5}$$

The new amplitudes $\tilde{t}^i_a$ that are associated with the single excitations used for this purpose can either be set equal to the conventional cluster amplitudes t^i_a, or be optimized independently ($\mathrm{XSP_{opt}}$ ansatz).

While these approaches aim at enhancing the description of correlation effects especially for small or medium sized basis sets, they are not expected to substantially correct basis set errors that arise in one-electron contributions. As proposed in Ref. 18, the latter may be achieved by exploiting the complementary auxiliary basis set (CABS), which is anyway needed for the evaluation of integrals containing the correlation factor (*vide infra*). Following Ref. 13, we supplement the conventional one-electron excitation operator T_1 with an operator

$$T_{1'} = t^{i}_{p''}a^{p''}_{i}, \tag{6}$$

which includes single excitations into the complementary virtual orbital space spanned by the auxiliary basis functions.

Combining this correction with $\mathrm{XSP_{opt}}$, we can write the cluster operator of the most flexible ansatz among the discussed ones as

$$S_{\mathrm{XSP_{opt}}+T_{1'}} = T + \mathcal{R} + [\mathcal{R},\tilde{T}_1] + T_{1'}. \tag{7}$$

Note that throughout this paper, S contains the correlation factor only in form of two-electron excitation operators. When CCSDT or CCSDTQ methods are used, higher excitations are only included by the conventional operators T_3 and T_4, whereas operators such as $[\mathcal{R},T_2]$ are not considered. For the use of such operators in the context of CCSD(T), see Ref. 21.

In the case of the full CCSD-F12 model, only terms linear and quadratic in $\mathcal{R}$ appear in the Lagrange functional $\mathcal{L}$. In this work, we will use the truncated CCSD(F12) model,[22–24] in which $\mathcal{L}$ is confined to terms that are at most linear in $\mathcal{R}$ and second-order in $\mathcal{R}$, $\mathcal{R}^\dagger$ and the two-electron part of the Hamiltonian. If the strong orthogonality projector $\mathcal{Q}_{12}$ is chosen as in ansatz 1 or 3 (modified ansatz 2), the CCSD(F12) model leads to the correct CCSD basis set limit and has been confirmed to be a very good approximation to the full model.[25,26] Following Ref. 13, we treat $T_{1'}$ on the same footing as $\mathcal{R}$. Computer generated explicit expressions for the Lagrangians of these methods can be found in the appendix of Ref. 13. When using higher excitations, we will employ a generalized CC(F12) model based on the same truncation criterion. Further truncations, which lead to less time-consuming F12 methods, will be discussed in Sec. II D.

B. Response theory

In the following we employ the quasienergy Lagrange formalism of response theory as introduced by Christiansen *et al.*[2] In order to describe the response of an atom or molecule to oscillating external fields, the Hamiltonian is written as a sum of the time-independent Hamiltonian H_0 for the unperturbed system, and a periodic perturbation $V(t) = V(t+\tau)$, which may be decomposed into Fourier components, each containing a field strength amplitude $\epsilon_i(\omega_i)$, associated with a frequency ω_i and a time-independent Hermitian operator X_i:

$$H(t) = H_0 + V(t) = H_0 + \sum_i \epsilon_i e^{-i\omega_i t}X_i. \tag{8}$$

Starting from the time-dependent Schrödinger equation and a coupled-cluster ansatz, Eq. (1), in which all optimized amplitudes are chosen to depend on time, we can derive a time-dependent quasienergy Lagrangian that is stationary with respect to a variation of the time-dependent cluster amplitudes t and Lagrange multipliers λ. For the most general ansatz $\mathrm{XSP_{opt}}+T_{1'}$ within the CC(F12) model, we obtain

$$\begin{aligned}\mathcal{L}_{\mathrm{XSP_{opt}}+T_{1'}} = {}& \langle 0|(1+\Lambda)(\bar{H} + [\bar{H},T_{1'} + \mathcal{R} + [\mathcal{R},\tilde{T}_1]])|0\rangle + \langle 0|(\Lambda_{1'} + \mathcal{R}^\dagger + [\tilde{\Lambda}_1,\mathcal{R}^\dagger])(\bar{H} + [F+V,T_{1'} + \mathcal{R} + [\mathcal{R},\tilde{T}_1]])|0\rangle \\ & - i\langle 0|\Lambda\frac{\partial T}{\partial t} + \Lambda_{1'}\frac{\partial T_{1'}}{\partial t} + [\tilde{\Lambda}_1,\mathcal{R}^\dagger]\left[\mathcal{R},\frac{\partial \tilde{T}_1}{\partial t}\right]|0\rangle,\end{aligned} \tag{9}$$

where

$$\bar{H} = e^{-T}(H_0 + V)e^{T}, \tag{10}$$

$$\Lambda = \sum_{i=1}^{N}\Lambda_i = \lambda^a_i a^i_a + \frac{1}{4}\lambda^{ab}_{ij}a^{ij}_{ab} + \cdots, \tag{11}$$

TABLE I. Definition of integrals and intermediates, symmetrization operators and projectors. σ_p denotes the m_s quantum number of the spin-orbital with index p, $\mathcal{P}_{pq}$ interchanges orbital indices p and q, and $\mathcal{Q}_{12}$ is the strong-orthogonality projector. For an explicit definition of $\mathcal{Q}_{12}$, see Eq. (21). o, v, and p project onto the occupied (i,j), virtual (a,b), and finite (p,q,r,s,t,u) orbital spaces; x projects onto virtual orbitals in the complementary space spanned by auxiliary basis functions (p'',q''). p' indexes orbitals in the union of the spaces given by p and x. α and β denote virtual orbitals in a complete basis.

$F_p^q = \langle p\|F(1)\|q\rangle$	$G_{pq}^{rs} = \langle pq\|r_{12}^{-1}\|rs\rangle$
$X_p^q = \langle p\|X(1)\|q\rangle$	
$\mathcal{R}_{\alpha\beta}^{pq} = \mathcal{S}_{pq}\langle \alpha\beta\|\mathcal{Q}_{12}f(r_{12})\|pq\rangle$	$R_{pq}^{rs} = \mathcal{S}_{rs}\langle pq\|f(r_{12})\|rs\rangle$
$(R^2)_{pq}^{rs} = \mathcal{S}_{pq}\mathcal{S}_{rs}\langle pq\|f^2(r_{12})\|rs\rangle$	$(\bar{R}^X)_{pq}^{rs} = R_{pq}^{p's}X_{p'}^{r} + R_{pq}^{rp'}X_{p'}^{s}$
$\mathcal{X}_{pq}^{rs} = \mathcal{S}_{pq}\mathcal{S}_{rs}\langle pq\|f(r_{12})\mathcal{Q}_{12}f(r_{12})\|rs\rangle$	
$\mathcal{V}_{pq}^{rs} = \mathcal{S}_{rs}\langle pq\|r_{12}^{-1}\mathcal{Q}_{12}f(r_{12})\|rs\rangle$	
$\mathcal{C}_{ab}^{pq} = \mathcal{S}_{pq}\langle ab\|[F(1)+F(2)]\mathcal{Q}_{12}f(r_{12})\|pq\rangle$	
$\mathcal{B}_{pq}^{rs} = \mathcal{S}_{pq}\mathcal{S}_{rs}\langle pq\|f(r_{12})\mathcal{Q}_{12}[F(1)+F(2)]\mathcal{Q}_{12}f(r_{12})\|rs\rangle$	
$(\mathcal{C}^X)_{ab}^{pq} = \mathcal{S}_{pq}\langle ab\|[X(1)+X(2)]\mathcal{Q}_{12}f(r_{12})\|pq\rangle$	
$(\mathcal{B}^X)_{pq}^{rs} = \mathcal{S}_{pq}\mathcal{S}_{rs}\langle pq\|f(r_{12})\mathcal{Q}_{12}[X(1)+X(2)]\mathcal{Q}_{12}f(r_{12})\|rs\rangle$	
$(\mathcal{B}_{\mathrm{I}}^X)_{pq}^{rs} = \mathcal{S}_{pq}\mathcal{S}_{rs}\langle pq\|f(r_{12})[X(1)+X(2)]\mathcal{Q}_{12}f(r_{12})\|rs\rangle$	
$(\mathcal{B}_{\mathrm{II}}^X)_{pq}^{rs} = \mathcal{S}_{pq}\mathcal{S}_{rs}\langle pq\|f(r_{12})[o_1X(1)+o_2X(2)]\mathcal{Q}_{12}f(r_{12})\|rs\rangle$	
$\mathcal{S}_{pq} = \frac{1}{4}(1-\mathcal{P}_{pq})$ if $\sigma_p = \sigma_q$	$\mathcal{S}_{pq} = \frac{1}{8}(3+\mathcal{P}_{pq})$ if $\sigma_p \neq \sigma_q$
$o = \Sigma_i \|i\rangle\langle i\|$	$v = \Sigma_a \|a\rangle\langle a\|$
$p = \Sigma_r \|r\rangle\langle r\|$	$x = \Sigma_{p''} \|p''\rangle\langle p''\|$

$$\tilde{\Lambda}_1 = \tilde{\lambda}_i^a a_a^i \overset{\mathrm{XSP}}{=} \lambda_i^a a_a^i, \tag{12}$$

$$\Lambda_{1'} = \lambda_i^{p''} a_{p''}^i, \tag{13}$$

and it is understood that V and all t and λ parameters depend on time. Merging these parameters into vectors $\boldsymbol{t}$ and $\boldsymbol{\lambda}$, the last part of Eq. (9) may be written as

$$-i\langle 0|\Lambda\frac{\partial T}{\partial t} + \Lambda_{1'}\frac{\partial T_{1'}}{\partial t} + [\tilde{\Lambda}_1,\mathcal{R}^\dagger]\left[\mathcal{R},\frac{\partial \tilde{T}_1}{\partial t}\right]|0\rangle = -i\boldsymbol{\lambda}\boldsymbol{S}\frac{\partial \boldsymbol{t}}{\partial t}, \tag{14}$$

with $\boldsymbol{S}$ denoting an overlap matrix. $\boldsymbol{S}$ is unity except for elements that arise from the XSP ansatz.

The real part of the time average of the Lagrangian,

$$\{\mathcal{L}\}_\tau = \frac{1}{\tau}\int_{t_0}^{t_0+\tau}\mathcal{L}(t)dt, \tag{15}$$

is the so-called quasienergy, once the stationary condition $\delta\{\mathcal{L}\}_\tau = 0$ is fulfilled. Derivatives thereof with respect to a set of field strength amplitudes yield frequency-dependent response functions:

$$\langle\langle X_1;X_2,\ldots,X_n\rangle\rangle_{\omega_2,\ldots,\omega_n} = \frac{1}{2}C^{\pm\omega}\left.\frac{d^n\Re\{\mathcal{L}\}_\tau}{d\epsilon_1 d\epsilon_2\cdots d\epsilon_n}\right|_{\epsilon=0}, \tag{16}$$

where the frequencies fulfill the condition $\omega_1+\cdots+\omega_n=0$ and the operator $C^{\pm\omega}$ symmetrizes the derivatives according to $C^{\pm\omega}f(\omega_i)=f(\omega_i)+f(-\omega_i)^*$, thus ensuring the symmetry of the response functions with respect to simultaneous sign inversion of all frequencies and complex conjugation. Choosing $n=0$, the energy of the unperturbed system may be retrieved from Eq. (16); $n=1$ results in the unperturbed expectation value of X_1.

The time-dependent cluster amplitudes and Lagrange multipliers are parametrized using Fourier expansions of the form

$$\boldsymbol{t} = \boldsymbol{t}_0 + \sum_i \epsilon_i e^{-i\omega_i t}\boldsymbol{t}^{X_i} + \frac{1}{2}\sum_{ij}\epsilon_i\epsilon_j e^{-i(\omega_i+\omega_j)t}\boldsymbol{t}^{X_iX_j} + \cdots, \tag{17}$$

where $\boldsymbol{t}_0$, $\boldsymbol{t}^{X_i}$, $\boldsymbol{t}^{X_iX_j}$, etc., are time-independent components associated with a set of frequencies and perturbation operators. By requiring $\{\mathcal{L}\}_\tau$ to be stationary with respect to these Fourier components of $\boldsymbol{t}$ and $\boldsymbol{\lambda}$, linear response equations can be derived, which allow a recursive calculation of those parameters:

$$(\mathbf{A}+\omega_k\boldsymbol{S})\boldsymbol{t}^{X_1\cdots X_{k-1}} = -\boldsymbol{\zeta}_t^{X_1\cdots X_{k-1}}, \tag{18}$$

$$\boldsymbol{\lambda}^{X_1\cdots X_{k-1}}(\mathbf{A}-\omega_k\boldsymbol{S}) = -\boldsymbol{\zeta}_\lambda^{X_1\cdots X_{k-1}}, \tag{19}$$

with $\omega_1+\cdots+\omega_k=0$. $\mathbf{A}$ is the Jacobi matrix and only depends on the zeroth-order cluster amplitudes $\boldsymbol{t}_0$, while $\boldsymbol{\zeta}_t$ and $\boldsymbol{\zeta}_\lambda$ denote expressions that contain cluster amplitudes of lower, or in the case of $\boldsymbol{\zeta}_\lambda$, equal order. Only in zeroth order, Eq. (18) becomes nonlinear and identical to the coupled-cluster equations.

C. Special F12 intermediates

When explicitly working out the expressions for the Lagrangians and their derivatives, terms containing three- and four-electron integrals arise due to the correlation factor. The special intermediates $\mathcal{X}$, $\mathcal{V}$, $\mathcal{C}$, and $\mathcal{B}$, listed in Tab. I, can be approximated by the usual techniques.[7,8] In course of response theory with one-electron perturbation operators X, two additional intermediates $\mathcal{C}^X$ and $\mathcal{B}^X$ arise, which resemble $\mathcal{C}$ and $\mathcal{B}$, but contain the perturbation instead of the Fock operator. Since ansatz 3, approximation C, is used throughout this work, $\mathcal{C}^X$ can simply be evaluated like the conventional $\mathcal{C}$ intermediate:

$$(\mathcal{C}^X)^{pq}_{ab} = X^{p''}_a R^{pq}_{p''b} + X^{p''}_b R^{pq}_{ap''}. \tag{20}$$

In the case of $\mathcal{B}^X$, two different techniques are used in this work. Similar to the treatment of $\mathcal{B}^X$ in ansatz 1 by Neiss and Hättig,[9] we can use direct resolution of the identity (RI) approximations by replacing both $\mathcal{Q}_{12}$ projectors with

$$\mathcal{Q}_{12} = (1 - p_1)(1 - p_2)(1 - v_1 v_2) \approx v_1 x_2 + x_1 v_2 + x_1 x_2, \tag{21}$$

where the projectors p, v, and x are defined in Table I.

Another approach is to treat $\mathcal{B}^X$ in the same way as $\mathcal{B}$ in approximation C.[7] Using

$$\mathcal{Q}_{12} = 1 - \mathcal{P}_{12} = 1 - o_1 - o_2 - v_1 v_2, \tag{22}$$

and the definitions from Table I, we can write $\mathcal{B}^X$ as[27]

$$(\mathcal{B}^X)^{rs}_{pq} = (\mathcal{B}^X_{\mathrm{I}})^{rs}_{pq} - (\mathcal{B}^X_{\mathrm{II}})^{rs}_{pq} - R^{ab}_{pq}(\mathcal{C}^X)^{rs}_{ab}. \tag{23}$$

While both $\mathcal{B}^X_{\mathrm{II}}$ and $\mathcal{C}^X$ are approximated using Eq. (21), we replace the remaining $\mathcal{Q}_{12}$ projector in $\mathcal{B}^X_{\mathrm{I}}$ with

$$\mathcal{Q}_{12} = 1 - \mathcal{P}_{12} \approx 1 - p_1 p_2 - o_1 x_2 - x_1 o_2. \tag{24}$$

To the term arising from the unit operator, we now apply the commutator relation $[f(r_{12}), X(1)+X(2)]=0$. This is valid if X is a position, momentum, or angular momentum operator which are the operators used in this work. Inserting approximate resolutions of the identity in order to separate the correlation factor from the perturbation operator, we finally arrive at

$$\begin{aligned}(\mathcal{B}^X_{\mathrm{I}})^{rs}_{pq} = {} & X^{p'}_p (R^2)^{rs}_{p'q} + X^{p'}_q (R^2)^{rs}_{pp'} - (\bar{R}^X)^{tu}_{pq} R^{rs}_{tu} - (\bar{R}^X)^{ip''}_{pq} R^{rs}_{ip''} \\ & - (\bar{R}^X)^{p''i}_{pq} R^{rs}_{p''i}.\end{aligned} \tag{25}$$

The latter approach consistently yields analytic derivatives of $\mathcal{B}$ with respect to the perturbation and will generally lead to a straighter convergence with increasing maximum l quantum number of the auxiliary basis set.

D. Simplified F12 methods

The special intermediates discussed in the previous section do not contain any t or λ parameters and therefore only need to be evaluated once in a computation. Within ansatz 2 or 3, additional terms containing the correlation factor arise. They are usually approximated by Eq. (21), yielding expressions such as $F^{p''}_i \lambda^a_j R^{ij}_{ap''}$ or $\lambda^a_k G^{kp''}_{ij} R^{ij}_{ap''}$, which require single contractions over auxiliary basis functions. We generally expect these terms to be small or to converge quickly to zero with increasing basis set size,[28] and therefore introduce a new approach in which they are omitted altogether. This is simply done by restricting the Lagrangian of a specific F12 method to conventional terms and terms containing one of the special intermediates $\mathcal{X}$, $\mathcal{V}$, $\mathcal{C}$, $\mathcal{B}$, $\mathcal{C}^X$, and $\mathcal{B}^X$. While this truncation of the Lagrangian will not necessarily lead to a systematic decline in accuracy, a huge gain in computational efficiency can be achieved, since no contractions over auxiliary basis functions will be needed after the evaluation of the special intermediates (except for terms containing $T_{1'}$). Therefore, in this work we will make use of this approximation and denote the respective F12 methods with a prime. We note that comparable simplifications introduced in the context of CCSD(T)-F12 by Werner and co-workers have already been proven to be successful.[18,19]

III. RESULTS

A. Computational details

Hartree–Fock reference determinants and integrals have been calculated by a local version of the DALTON[29] program. The GECCO program, which has been employed earlier for the computation of excitation energies using the discussed F12 methods,[13] has been equipped with a tool to automatically derive response equations of arbitrary order, starting from a method dependent zeroth-order Lagrangian. GECCO features a symbolic operator algebra and a string-based evaluation of terms. Details about the implementation will be reported elsewhere. Currently, the response module supports conventional coupled-cluster methods and a variety of F12 methods based on the SP and XSP approaches. Arbitrary frequency-dependent response functions containing one-electron operators may be computed. This has been verified for dynamic electrical properties up to second hyperpolarizabilities and for optical rotations both in the length and modified velocity formulations. For the latter, the DALTON program has been employed when computing self-consistent field (SCF) and conventional CCSD results.

A Slater-type correlation factor,

$$f(r_{12}) = \frac{1}{\gamma} e^{-\gamma r_{12}}, \tag{26}$$

with the interelectronic distance r_{12} and a length scale parameter that was chosen as $\gamma = 1.4 a_0^{-1}$ has been used throughout this work. It was approximated by six Gaussians, using the parameters from Ref. 15.

Details about the choice of coordinates and basis sets employed are listed in Table II. F12 intermediates were evaluated within ansatz 3, approximation C,[7] making use of the CABS approach.[30] One exception is the special intermediate $\mathcal{B}^X$, which in some cases has been evaluated by an approximate resolution of the identity. This was done in the case of LiF and H_2O_2 where the frozen core approximation was used which was not yet available for the reformulated $\mathcal{B}^X$. In case of the $\mathrm{XSP}'_{\mathrm{opt}}$ calculations for the N_2 molecule, the use of the reformulated $\mathcal{B}^X$ triggered some numerical problems when solving the response equations. This issue remains to be further analyzed, in particular, linear dependencies in the geminal basis call for a more stable response solver for the $\mathrm{XSP}_{\mathrm{opt}}$ ansatz.

Besides problems in this specific case, both techniques for evaluating $\mathcal{B}^X$ have been found to yield response functions agreeing within 0.1%, showing that the choice between the two is not a critical one. However, as expected the evaluation according to approximation C yields a much straighter convergence with increasing maximum l quantum number of the auxiliary basis set, examples are given in Table S1 of the supplementary material.[31]

TABLE II. Computational details. Structural parameters have been adopted from Ref. 13 (BH), Ref. 32 (LiF), Ref. 9 (N_2), and Ref. 37 (H_2O_2). The coordinates of BH and LiF were chosen such that the z axis points from the heavier to the lighter nucleus. In the case of H_2O_2, the origin is at the center of mass. Augmented correlation consistent Dunning basis sets as described in Refs. 38 and 39 have been employed. The basis sets $19s14p8d6f4g3h2i$ and $21s14p7d6f5g4h3i$ are described in Refs. 40 and 13, respectively.

Molecule	Structural parameters	Frozen core	Basis set	Auxiliary basis set (decontracted)
BH	$r_{\mathrm{BH}}=2.328\,898\,31a_0$	—	aug-cc-pVXZ, $X=D,\ldots,5$	aug-cc-pV($X+1$)Z
			aug-cc-pV6Z	$19s14p8d6f4g3h2i$
LiF	$r_{\mathrm{LiF}}=2.955\,274\,67a_0$	$1s_{\mathrm{F}}^2 1s_{\mathrm{Li}}^2$	d-aug-cc-pVXZ, $X=$D,T,Q	$21s14p7d6f5g4h3i$
N_2	$r_{\mathrm{NN}}=2.074\,000\,00a_0$	—	d-aug-cc-pVXZ, $X=$D,$\ldots$,5	d-aug-cc-pV($X+1$)Z
			t-aug-cc-pVXZ, $X=$D,$\ldots$,5	t-aug-cc-pV($X+1$)Z
			n-aug-cc-pV6Z, $n=$d,t	$19s14p8d6f4g3h2i$
H_2O_2	$r_{\mathrm{OO}}=2.626\,719\,33a_0$	$1s_{\mathrm{O}_1}^2 1s_{\mathrm{O}_2}^2$	H: aug-cc-pVXZ, $X=$D,$\ldots$,5	cc-pVTZ for $X=$D,Q
	$r_{\mathrm{OH}}=1.776\,343\,14a_0$		O: s,p,d-type functions: d-aug-cc-pVXZ	cc-pVQZ for $X=$T
	$\angle_{\mathrm{HOH}}=102.3°$		O: f,g,h-type functions: cc-pVXZ	

B. Static electrical properties of BH

Static electrical properties of BH were calculated in order to assess the CCSD(F12) methods using the ansätze SP, XSP, XSP′, $\mathrm{XSP}'_{\mathrm{opt}}$, and $\mathrm{XSP}'_{\mathrm{opt}}+T_{1'}$. For an analysis of the basis set convergence, we split the response functions into a pure one-electron and a correlation contribution according to the Lagrangians

$$\mathcal{L}^{\text{one-el.}} = \langle 0|(1+\Lambda_1)e^{-T_1}He^{T_1}|0\rangle, \tag{27}$$

$$\mathcal{L}^{\text{corr.}} = \mathcal{L} - \mathcal{L}^{\text{one-el.}}. \tag{28}$$

Since $\mathcal{L}^{\text{one-el.}}$ has the same form as $\mathcal{L}_{\text{CCS}}$, CCS results will be included in the analysis. When the $T_{1'}$ extension is used, $\mathcal{L}^{\text{one-el.}}$ also comprises the respective terms containing operators $\Lambda_{1'}$ and $T_{1'}$. We note that in calculations using the above described analysis of the Lagrangian, the $2n+1$ ($2n+2$) rules must not be applied in order to avoid unintended coupling between $\mathcal{L}^{\text{one-el.}}$ and $\mathcal{L}^{\text{corr.}}$. All data corresponding to the figures of the current section may be found in the supplementary material (Tables S2–S4).[31]

The basis set convergence of the dipole moment μ_z and its one-electron contribution $\mu_z^{\text{one-el.}}$ is shown in Fig. 1. All of the considered F12 methods greatly accelerate the convergence. Both SP and $\mathrm{XSP}'_{\mathrm{opt}}$ even appear to be effectively converged at the aug-cc-pVTZ level. The small error of the XSP and XSP′ ansätze which is caused by using the same set of parameters both in one- and two-electron (de)excitation operators diminishes slowly with increasing basis set size but can be avoided altogether by using two independent sets of parameters as done in the $\mathrm{XSP}'_{\mathrm{opt}}$ ansatz. Generally, for XSP and XSP′ results, a good agreement is found that justifies the use of the simplified F12 methods. This will further be elaborated at the end of the present section. The $T_{1'}$ option efficiently corrects $\mu_z^{\text{one-el.}}$ for small basis sets. However, since the one-electron basis set error is small and happens to cancel a part of the correlation basis set error, no net improvement is obtained in this case.

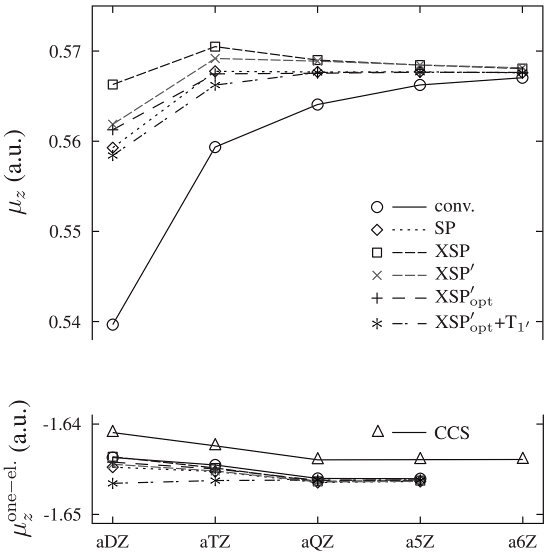

FIG. 1. BH: dipole moment μ_z and its one-electron contribution, values in atomic units computed using CCSD methods and aug-cc-pVXZ basis sets.

The basis set convergence of the components α_{zz} and α_{xx}, presented in Fig. 2, confirms that the original SP approach is not generally well suited for response theory. While it is still able to improve α_{zz} compared to conventional CCSD, it fails in the more challenging case of α_{xx}, which requires explicitly correlated functions of π symmetry. Those functions are missing in the SP approach as a consequence of all occupied orbitals of BH being totally symmetric. The same problem has already been found for the CCSD(R12)

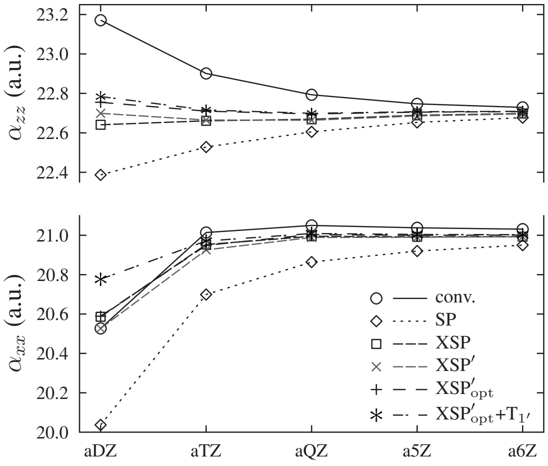

FIG. 2. BH: components α_{zz} and α_{xx} of the static polarizability of BH, values in atomic units computed using CCSD methods and aug-cc-pVXZ basis sets.

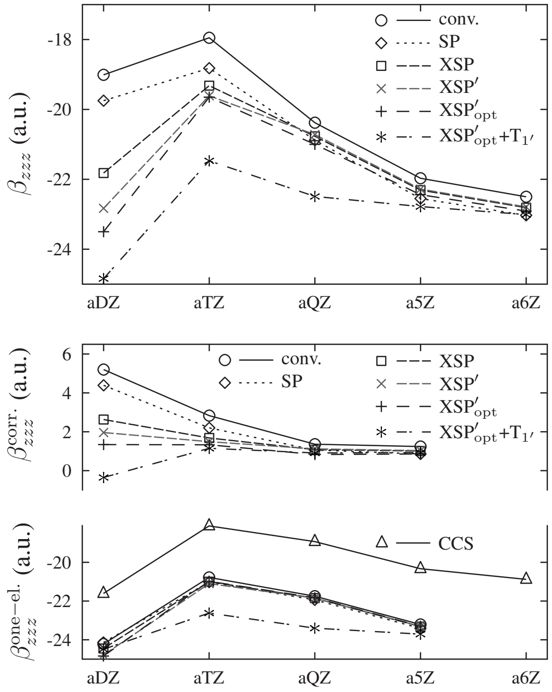

FIG. 3. BH: static hyperpolarizability β_{zzz} (upper panel) and its one-electron and correlation contributions, values in atomic units computed using CCSD methods and aug-cc-pV*XZ* basis sets.

method and could be solved by including three selected virtual orbitals to the R12 space,[9] a strategy similar to the extended approach XSP. Indeed, the XSP ansatz corrects this deficiency by letting the correlation factor act on occupied-virtual orbital pairs as well. Further improvement and a rapid convergence of α_{zz} can be obtained with XSP$'_{\text{opt}}$. In the case of α_{xx}, even conventional CCSD leads to excellent results for aug-cc-pVTZ and aug-cc-pVQZ basis sets, but the remaining basis set error diminishes only slowly with increasing basis set size. This may be concluded from the great stability of XSP$'_{\text{opt}}$ results for large basis sets which indicates that the basis set limit is close to these values. The convergence of the correlation contribution was found to be predominant for α_{zz}, while in the case of α_{xx} the convergence of both contributions is of equal importance for small basis sets. As a consequence, the $T_{1'}$ option accelerates the convergence of α_{xx} to some extent.

A case in which the total convergence behavior is mainly determined by the one-electron contribution is the component β_{zzz} of the hyperpolarizability of BH, as can be seen in Fig. 3. While $\beta^{\text{corr.}}_{zzz}$ is systematically improved by the ansätze SP, XSP, and XSP$'_{\text{opt}}$ as expected, a correction of the one-electron basis set error is crucial for achieving significant improvements. Though the $T_{1'}$ extension is able to greatly reduce the one-electron error, there is still need for more efficient methods aimed at improving the one-electron contribution.

Comparison of XSP and XSP′ shows that terms containing the correlation factor other than in the form of $\mathcal{X}$, $\mathcal{V}$, $\mathcal{C}$, $\mathcal{B}$, $\mathcal{C}^X$, and $\mathcal{B}^X$ may safely be neglected when using large basis sets. Significant, but minor, deviations of less than 1% for μ and α only occur when using aug-cc-pVDZ and aug-cc-pVTZ basis sets, while for larger basis sets XSP and XSP′ results only differ by up to 0.03%. In the case of β_{zzz} the relative deviations between XSP and XSP′ are about 5% for aug-cc-pVDZ and less than 0.3% for aug-cc-pVQZ and larger basis sets, but at the same time the basis set errors of all the discussed methods are also relatively larger, thus confirming the usefulness of the simplified F12 methods.

Figures 1 and 3 indicate that the convergence behavior of the one-electron contribution of methods which do not employ a $T_{1'}$ option strongly resembles the convergence of the CCS values, roughly shifted by a constant. This will allow us to get an idea about the convergence of correlation contributions of response properties by simply subtracting the CCS result obtained using the same basis sets.

C. Static hyperpolarizability β_{zzz} of LiF

The static hyperpolarizability β_{zzz} of LiF has been found to exhibit a slow convergence to the correlation limit within the coupled-cluster series.[32] Accurate calculations require the use of quadruple excitations. Because CCSDTQ calculations are only feasible for small basis sets, F12 methods including higher-order excitations might be used in order to obtain results close to the basis set limit.

Table III contains CCSD(F12) and CCSDT(F12) results obtained employing ansätze SP and XSP as well as CCSD(F12)-XSP+$T_{1'}$ results. Note that in the context of this paper, CCSDT(F12)-SP (CCSDTQ(F12)-SP) refers to an extension of CCSD(F12)-SP in which the cluster operator has been augmented by conventional triple (and quadruple) excitations. No explicitly correlated higher-order excitation operators are considered.

Both for CCSD(F12) and CCSDT(F12) the SP and XSP results are almost identical (within 0.2%) and exhibit a faster basis set convergence than the conventional values. Interpreting the difference to the CCS values of the same basis set as a measure for the correlation contribution, the

TABLE III. LiF: static hyperpolarizability β_{zzz} in atomic units, computed using d-aug-cc-pV*XZ* basis sets. CCSD values relative to CCS are given in parentheses. In the case of CCSDT, increments with respect to the corresponding CCSD methods are given in parentheses.

		CCSD				CCSDT		
XZ	CCS	Conv.	SP	XSP	XSP+$T_{1'}$	Conv.	SP	XSP
DZ	−15.61	−33.90(−18.29)	−28.85(−13.24)	−28.82	−26.70	−35.17(−1.27)	−29.51(−0.66)	−29.48
TZ	−14.50	−29.67(−15.17)	−27.58(−13.08)	−27.55	−27.33	−31.48(−1.81)	−29.03(−1.45)	−29.01
QZ	−14.16	−28.12(−13.96)	−27.21(−13.05)	−27.21	−27.32	−30.06(−1.94)	−28.98(−1.77)	−28.99

TABLE IV. Hyperpolarizability β_{zzz} of LiF: total CCSD results in atomic units, CCSDT (CCSDTQ) results given as increments with respect to CCSD (CCSDT). d-aug-cc-pV*XZ* basis sets have been used.

	Conv.		SP′		SP′+$T_{1'}$	
	DZ	TZ	DZ	TZ	DZ	TZ
CCSD	−33.90	−29.67	−28.94	−27.66	−26.79	−27.48
ΔCCSDT	−1.27	−1.81	−0.61	−1.46	−0.53	−1.39
ΔCCSDTQ	1.38	1.27	1.08		1.00	

CCSD(F12)-SP [and CCSD(F12)-XSP] correlation contribution converges quickly and leads to a practically converged β_{zzz} with the CCSD(F12)-XSP+$T_{1'}$ method using d-aug-cc-pVTZ. Assuming a convergence behavior of $\sim X^{-3}$ for conventional CCSD, the basis set limit of the difference between CCS and CCSD can be estimated as −13.1 ± 0.4, where the uncertainty is estimated as half the difference between the d-aug-cc-pVQZ result and the basis set limit. While this limit agrees well with the values obtained with SP or XSP, the uncertainty is more than ten times higher than the difference between the d-aug-cc-pVTZ and d-aug-cc-pVQZ correlation contributions for SP or XSP. Since for XSP the $T_{1'}$ extension leads to a positive correction for d-aug-cc-pVTZ but to a negative correction for d-aug-cc-pVQZ it is not clear whether the convergence of the one-electron contribution is monotonous beyond the d-aug-cc-pVQZ basis set. Thus, in order to compute an estimate for the total basis set limit based on conventional results, we simply employ the CCS value obtained with d-aug-cc-pVQZ with an estimated uncertainty of ±0.2 (half the difference between the d-aug-cc-pVTZ and d-aug-cc-pVQZ results), arriving at a total CCSD basis set limit of −27.3 ± 0.5, which agrees with the practically converged XSP+$T_{1'}$ values.

Within CCSDT(F12), stable results for the d-aug-cc-pVTZ and d-aug-cc-pVQZ basis sets can be obtained even without the $T_{1'}$ option, indicating compensation of one-electron and correlation basis set errors. However, the difference between CCSD and CCSDT results appears to converge slower for the SP and XSP approaches than for conventional coupled cluster. We interpret this as a consequence of treating double and triple excitations on a different footing within the presently used CCSDT(F12) methods, i.e., by leaving out the explicitly correlated excitation operator $[\mathcal{R},T_2]$. Nevertheless, adding the difference between conventional CCSD and CCSDT results obtained using d-aug-cc-pVQZ to the estimated CCSD limit yields an estimate of −29.2 for the CCSDT limit, which agrees well with the CCSDT(F12)-SP [and CCSDT(F12)-XSP] results for the medium-sized basis sets.

When turning to quadruple excitations, we resort to the less time consuming SP′ and SP′+$T_{1'}$ ansätze. Table IV contrasts the d-aug-cc-pVDZ results for these two approaches at the CCSD, CCSDT, and CCSDTQ level of theory with conventional results. d-aug-cc-pVTZ values are also reported for CCSD and CCSDT methods. Comparing the SP′ results of this table with the respective SP values from Table III, we find deviations of less than 0.1 a.u. (≈0.3%), which is again evidence for the effectiveness of the simplifications used in the SP′ ansatz. The CCSDT-CCSDTQ increments employing d-aug-cc-pVDZ for conventional coupled-cluster and F12 methods do not differ as dramatically as the CCSD-CCSDT increments, indicating that explicitly correlated operators of the type $[\mathcal{R},T_3]$ might be of low importance in the present example. The CCSDTQ basis set limit is expected to be close to the FCI limit.[32] A simple estimation based on conventional results by adding the difference between CCSDT and CCSDTQ for the d-aug-cc-pVTZ basis to the approximate CCSDT limit yields −27.9, which lies in between the corresponding SP′ and SP′+$T_{1'}$ results. This is in harmony with the trend that SP′ and SP′+$T_{1'}$ converge from opposite sides for small basis sets and we conclude that the SP′ result computed using d-aug-cc-pVDZ lies within a few percent of the CCSDTQ basis set limit while the conventional result obtained using the same basis set is about 20% too low.

D. Static electrical properties of N_2

Neiss and Hättig[9] calculated static polarizabilities and static as well as dynamic second hyperpolarizabilities of N_2 using the R12 method CCSD(R12), which lead to a faster basis set convergence compared to conventional CCSD in all cases. We now use the same system in order to assess the discussed F12 ansätze SP, XSP, XSP$'_{\text{opt}}$, and XSP$'_{\text{opt}}$+$T_{1'}$.

Tables V and VI contain results for the static properties α_{zz}, α_{xx}, and $\gamma_{\parallel}$. Basically, the expected trends as discussed above are confirmed. In the case of the polarizability, the SP approach performs even worse than conventional CCSD, whereas excellent results for α_{zz} and α_{xx} within 0.1% of the expected basis set limit as estimated in Ref. 9 can be obtained by XSP$'_{\text{opt}}$ using the basis sets d-aug-cc-pVTZ and d-aug-cc-pVQZ as well as by XSP when using d-aug-cc-pVQZ. In order to achieve this level of accuracy with CCSD(R12), one has to employ the larger basis sets d-aug-cc-pV5Z and d-aug-cc-pV6Z. For the basis sets of interest, the $T_{1'}$ option makes only little difference as we would expect based on the rapid convergence of the SCF results.

In our analysis of the parallel component of the second hyperpolarizability[33]

$$\gamma_{\parallel} = \frac{1}{15}\sum_{\xi\eta}(\gamma_{\xi\xi\eta\eta} + \gamma_{\xi\eta\eta\xi} + \gamma_{\xi\eta\xi\eta}), \qquad (29)$$

where $\xi,\eta = x,y,z$, we will employ the basis set limits as estimated by Neiss and Hättig for SCF (714.7 ± 0.2) and for the correlation contribution (148.6 ± 3.1), leading to a total limit of 863.3 ± 3.3. The differences between CCSD and SCF results obtained using the same basis sets are interpreted

TABLE V. N_2: component α_{zz} and α_{xx} of the static polarizability, values in atomic units computed using d-aug-cc-pV*XZ* basis sets.

		CCSD					
XZ	SCF[a]	Conv.[a]	(R12)[a]	SP	XSP	XSP'_{opt}	$\text{XSP}'_{\text{opt}}+T_{1'}$
				α_{zz}			
DZ	15.003	14.800	14.605	14.268	14.506	14.543	14.537
TZ	15.044	14.665	14.594	14.426	14.536	14.561	14.549
QZ	15.034	14.609	14.575	14.495	14.543	14.558	14.553
5Z	15.029	14.577	14.558	14.517			
6Z	15.028	14.565	14.549				
				α_{xx}			
DZ	9.774	10.212	10.064	9.808	9.964	10.005	10.032
TZ	9.834	10.174	10.112	9.989	10.063	10.082	10.080
QZ	9.835	10.130	10.100	10.041	10.075	10.084	10.083
5Z	9.832	10.106	10.089	10.058			
6Z	9.832	10.096	10.082				

[a] Values from Ref. 9.

as correlation contributions, except for $\text{XSP}'_{\text{opt}}+T_{1'}$, which is designed to additionally improve the one-electron contribution. Figure 4 shows the basis set errors of SCF, those of the correlation contributions for conventional CCSD, CCSD(R12), CCSD(F12)-SP, CCSD(F12)-XSP, CCSD(F12)-XSP'_{opt}, and the error of the total CCSD(F12)-$\text{XSP}'_{\text{opt}}+T_{1'}$ results with respect to the SCF, correlation and total basis set limits, but relative to the total basis set limit. In this way, Fig. 4 directly reveals how the correlation contribution is improved by the explicitly correlated methods while simultaneously showing the impact of the one-electron error. While conventional coupled-cluster, (R12), and XSP'_{opt} rather profit from cancellation of one-electron and correlation errors, for SP and XSP both contributions approach from below, ending up with a larger total error. The XSP'_{opt} ansatz however leads to more balanced and accurate results which for the basis sets d-aug-cc-pVQZ, t-aug-cc-pVTZ and t-aug-cc-pVQZ agree with the estimated basis set limit within the given uncertainty, see Table VI. It turns out that even the result for the basis set d-aug-cc-pVTZ mainly suffers from a rather slow convergence of the one-electron contribution as it is greatly improved by employing the $T_{1'}$ option. Only by using the large basis sets d-aug-cc-pV6Z and t-aug-cc-pV6Z can the same accuracy be achieved with the CCSD(R12) method.

E. Dynamic second hyperpolarizabilities of N_2

So far it has been shown that the XSP'_{opt} ansatz reliably leads to excellent results even for medium-sized basis sets such as t-aug-cc-pVTZ and t-aug-cc-pVQZ. To see whether this is also valid for frequency-dependent properties, we computed the dynamic electric field induced second harmonic generation (ESHG) hyperpolarizabilities $\gamma_{\parallel}^{\text{ESHG}}(\omega)=\gamma_{\parallel}(-2\omega;\omega,\omega,0)$ for several frequencies. Table VII also contains an estimate for the basis set limit which was calculated by scaling the CCSD(R12) results obtained with t-aug-cc-pVQZ with the ratio of the static CCSD(R12) results for t-aug-cc-pV6Z and t-aug-cc-pVQZ.[9] This quantity has suc-

TABLE VI. N_2: parallel component $\gamma_{\parallel}$ of the static second hyperpolarizability, values in atomic units computed using n-aug-cc-pV*XZ* basis sets with $n=\text{d},\text{t}$.

		CCSD					
XZ	SCF[a]	Conv.[a]	(R12)[b]	SP	XSP	XSP'_{opt}	$\text{XSP}'_{\text{opt}}+T_{1'}$
			d-aug-cc-pV*XZ*				
DZ	672.0	937.6	883.7	813.4	820.6	833.8	855.7
TZ	697.1	895.3	874.5	840.1	844.3	856.9	863.5
QZ	709.9	880.7	870.6	854.8	856.7	863.1	864.6
5Z	713.9	873.2	867.6	859.6			
6Z	714.4	869.2	864.5				
			t-aug-cc-pV*XZ*				
DZ	669.2	935.4	881.7	811.6	818.9	832.1	858.5
TZ	710.1	903.0	882.4	847.5	851.6	864.3	865.6
QZ	713.2	882.7	872.7	856.9	858.8	865.2	864.9
5Z	714.3	873.3	867.6				
6Z	714.7	869.5	864.5				

[a] Values from Ref. 41.
[b] Values from Ref. 9.

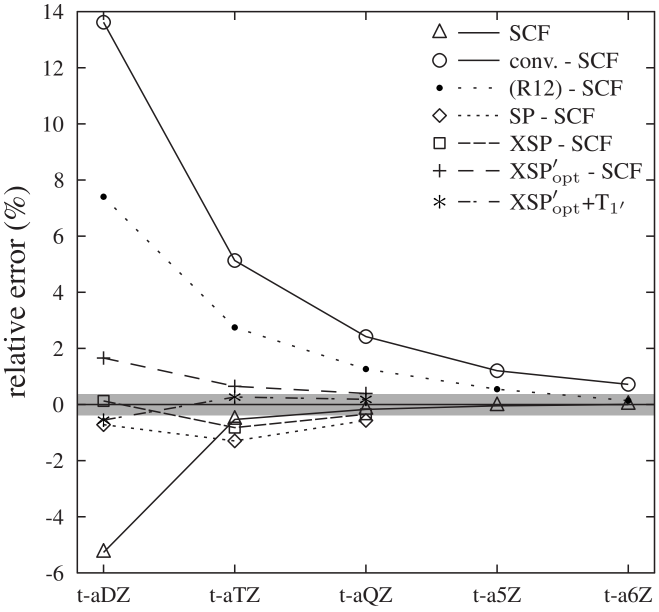

FIG. 4. Static second hyperpolarizability of N_2: relative basis set errors for SCF and for the correlation contributions (estimated as difference to the corresponding SCF result) obtained with conventional CCSD, CCSD(R12), CCSD(F12)-SP, CCSD(F12)-XSP, and CCSD(F12)-$\mathrm{XSP}'_{\mathrm{opt}}$ as well as for the total CCSD(F12)-$\mathrm{XSP}'_{\mathrm{opt}}+T_{1'}$ results. All values are given relative to the total basis set limit as estimated in Ref. 9, with the uncertainty of this limit indicated by the gray margin. t-aug-cc-pV*X*Z basis sets have been used.

cessfully been employed by Neiss and Hättig as a best estimate for the basis set limit in course of a computation of total $\gamma_{\parallel}^{\mathrm{ESHG}}(\omega)$ values including corrections for zero-point vibrational averaging and higher-order correlation effects, leading to a good agreement with experimental results. We find that the results obtained with CCSD-$\mathrm{XSP}'_{\mathrm{opt}}$ for the basis set t-aug-cc-pVQZ and even for t-aug-cc-pVTZ agree with the estimate from Ref. 9 within 0.1%, demonstrating that the $\mathrm{XSP}'_{\mathrm{opt}}$ ansatz also yields excellent results for dynamic properties. Figure 5 further illustrates the enhanced basis set convergence of explicitly correlated methods by showing dynamic ESHG hyperpolarizabilities relative to CCS for the basis sets t-aug-cc-pVTZ and t-aug-cc-pVQZ. Especially for $\mathrm{XSP}'_{\mathrm{opt}}$ the difference between the t-aug-cc-pVTZ and t-aug-cc-pVQZ correlation contributions remains small across the range of frequencies considered.

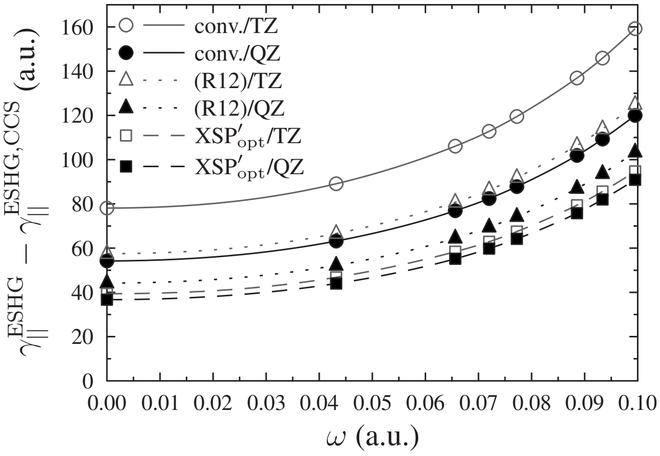

FIG. 5. N_2: parallel component $\gamma_{\parallel}^{\mathrm{ESHG}}(\omega)$ of the dynamic ESHG hyperpolarizability for CCSD methods relative to CCS, values in atomic units computed using t-aug-cc-pV*X*Z basis sets with $X=\mathrm{T},\mathrm{Q}$.

F. Optical rotation of H_2O_2

In order to demonstrate that our conclusions also apply to the calculation of response functions containing one-electron operators other than the position operator, we computed specific optical rotations,

$$[\alpha]_{\omega} = 28\,800\pi^2 N_{\mathrm{A}} a_0^4 \frac{\tilde{\nu}^2 \beta'(\omega)}{M}, \tag{30}$$

for H_2O_2, which constitutes an excellent test system for that purpose.[34] This was done at the frequency of the sodium *D*-line (589.3 nm, $\omega=0.077\,318$ a.u.) for two dihedral angles $\theta=50°$ and $\theta=110°$, and both in the length gauge formulation

$$\beta'(\omega) = -\Im \frac{\mathrm{Tr}\langle\langle \vec{r};\vec{L}\rangle\rangle_{\omega}}{6\omega}, \tag{31}$$

and in the modified velocity formulation

$$\beta'(\omega) = -\Re \frac{\mathrm{Tr}(\langle\langle \vec{p};\vec{L}\rangle\rangle_{\omega} - \langle\langle \vec{p};\vec{L}\rangle\rangle_{0})}{6\omega^2}, \tag{32}$$

where $\vec{r}$ denotes the position, $\vec{p}$ the momentum, and $\vec{L}$ the angular momentum operator; N_{A} is Avogadro's number, a_0 is the Bohr radius in cm, $\tilde{\nu}$ is the frequency in cm^{-1}, M is

TABLE VII. N_2: parallel component $\gamma_{\parallel}^{\mathrm{ESHG}}(\omega)$ of the dynamic ESHG hyperpolarizability, values in atomic units computed using t-aug-cc-pV*X*Z basis sets.

λ (nm)	ω (a.u.)	CCS TZ	CCS QZ[a]	CCSD(F12)-$\mathrm{XSP}'_{\mathrm{opt}}$ TZ	CCSD(F12)-$\mathrm{XSP}'_{\mathrm{opt}}$ QZ	CCSD(R12)[a] TZ	CCSD(R12)[a] QZ	Limit[a]
∞	0.000 000	824.9	828.5	864.3	865.2	882.4	872.7	864.5
1055.0	0.043 188	870.1	873.7	916.9	917.7	936.7	925.9	917.2
694.3	0.065 625	935.0	938.7	993.4	993.9	1015.7	1003.2	993.8
632.8	0.072 003	960.1	963.9	1023.2	1023.7	1046.6	1033.4	1023.7
590.0	0.077 226	983.3	987.0	1050.8	1051.2	1075.2	1061.3	1051.3
514.5	0.088 558	1042.7	1046.5	1122.1	1122.3	1149.1	1133.5	1122.8
488.0	0.093 368	1072.2	1076.0	1157.8	1158.0	1186.1	1169.7	1158.7
457.9	0.099 505	1114.2	1118.1	1208.9	1209.0	1239.1	1221.5	1210.0

[a] Values from Ref. 9, the limit has been estimated from the given CCSD(R12) results.

TABLE VIII. H_2O_2: optical rotations for two dihedral angles θ, values in deg[dm g/cm^3]$^{-1}$ computed using both length and modified velocity gauge formulations. The basis sets employed are modified Dunning basis sets as described in Table II and in the text.

		CCSD				
XZ	SCF	Conv.	SP′	XSP′	XSP'_{opt}	$XSP'_{opt}+T_{1'}$
			$\theta=50°$, length gauge			
DZ	69.43	161.38	123.79	133.58	133.06	129.40
TZ	68.03	137.69	122.78	125.66	127.39	126.38
QZ	67.40	129.71	122.79	123.88	124.96	125.48
5Z	67.26	126.87				
			$\theta=50°$, modified velocity gauge			
DZ	77.35	189.26	143.34	159.33	158.43	155.46
TZ	70.61	164.40	146.69	151.24	153.44	152.25
QZ	67.36	155.57	147.30	148.76	150.10	149.33
5Z	67.34	153.41				
			$\theta=110°$, length gauge			
DZ	32.24	−15.60	0.41	−0.42	0.06	−0.62
TZ	31.19	−5.91	0.67	0.65	−0.41	−1.21
QZ	29.71	−3.64	−0.40	−0.47	−1.23	−1.34
5Z	29.87	−2.27				
			$\theta=110°$, modified velocity gauge			
DZ	20.88	−53.25	−30.62	−34.27	−33.27	−31.79
TZ	27.88	−32.25	−23.80	−25.01	−26.18	−26.39
QZ	29.43	−27.30	−23.14	−23.86	−24.70	−24.32
5Z	29.79	−26.00				

the molecular weight in g/mol, and $[\alpha]_\omega$ is obtained in deg[dm g/cm^3]$^{-1}$. For theoretical background, we refer to Refs. 35 and 36, mentioning here only that both formulations agree in the limit of a complete basis set given that the orbitals are variationally optimized. While the latter applies to the methods SCF and full configuration interaction (FCI), truncated coupled-cluster methods generally yield differing results even for a complete basis.

We employed modified basis sets which in the context of this section will simply be denoted by *XZ*, $X=\mathrm{D},\ldots,5$. While aug-cc-pV*XZ* has been used for hydrogen, in the case of oxygen we abandoned the augmentation for high l quantum numbers but used the functions from the d-aug-cc-pV*XZ* basis for $l=0,1,2$. The choice of auxiliary basis sets, given in Table II, is motivated by a simple test using the BH molecule, which indicated that the augmentation of the auxiliary basis is not crucial and that at the QZ level a smaller auxiliary basis may be employed without causing considerable errors.

The basis set convergence of the SCF values, presented in Table VIII, shows that the common basis set limit for both gauge formulations is effectively obtained at the QZ level, with the length gauge results featuring much smaller basis set errors for the DZ and TZ basis sets. As we expect the XSP'_{opt} ansatz to efficiently correct the basis set error due to correlation, the QZ results obtained with XSP'_{opt} or $XSP'_{opt}+T_{1'}$ may serve as reasonable approximations for the CCSD basis set limits. This is also supported by the observation that, for $\theta=50°$, the $XSP'_{opt}+T_{1'}$ values are close to those conventional results obtained using the corresponding $(X+2)$Z basis. While the $T_{1'}$ extension leads to partial improvements at the DZ and TZ level in most cases, it is hardly able to improve $[\alpha]_D(\theta=110°)$ in modified velocity gauge despite substantial SCF errors for these basis sets. Even the simple SP′ ansatz leads to remarkable improvements compared to conventional CCSD, though this is partially due to compensation of one-electron and correlation errors, most clearly seen in the opposing trends of SP′ and SCF results in the case of $[\alpha]_D(\theta=50°)$ in modified velocity gauge.

Though the discussed F12 methods can be used to accelerate the basis set convergence, the problematic difference (in deg[dm g/cm^3]$^{-1}$) of about 25 units between the basis set limits obtained in the length and modified velocity gauge formulations can only be mended by including higher excitations into the cluster operator. While for the DZ basis the difference in $[\alpha]_D(\theta=110°)$ between length and modified velocity gauge is about 38 units for conventional CCSD and about 31 for CCSD(F12)-SP′, we obtained the conventional CCSDT results $[\alpha]_D(\theta=110°)=-15.93$ deg[dm g/cm^3]$^{-1}$ in length gauge and $[\alpha]_D(\theta=110°)=-38.63$ deg[dm g/cm^3]$^{-1}$ in modified velocity gauge as well as the CCSDT(F12)-SP′ values $[\alpha]_D(\theta=110°)=-0.02$ deg[dm g/cm^3]$^{-1}$ in length gauge and $[\alpha]_D(\theta=110°)=-20.57$ deg[dm g/cm^3]$^{-1}$ in modified velocity gauge, yielding smaller differences of about 23 and 21 units, respectively. As these deviations are still larger than the SCF difference of about 11 units, which is solely due to basis set incompleteness, we conclude that even higher excitations would be needed in order to harmonize both formulations. However, the inclusion of triple excitations hardly affects the length gauge result, indicating that length gauge would be the preferred choice in the present case.

IV. CONCLUSIONS

In the present work, we tested a variety of explicitly correlated coupled-cluster methods, which make use of the *s*- and *p*-wave cusp conditions and employ a Slater-type correlation factor $f(r_{12})$, for their applicability in the computation of static and dynamic response properties. We have shown how the intermediate $\mathcal{B}^X$ that contains the perturbation operator X may be evaluated within ansatz 3, approximation C, a procedure based on a vanishing commutator $[f(r_{12}),X(1)+X(2)]$. Employing the position, momentum, and angular momentum operators as perturbation, we computed static and dynamic electrical properties up to second hyperpolarizabilities, as well as optical rotations. In some examples, higher excitations up to quadruple excitations have been used in combination with the discussed F12 ansätze.

In many instances, even the basic SP approach was able to efficiently correct the correlation basis set error of conventional coupled-cluster methods. However, it severely failed in some cases, e.g., for the polarizabilities of BH and N_2, obviously due to the lack of geminal functions suited for the description of correlation effects induced by the perturbation. The XSP approach includes geminals generated by action of the correlation factor on singly excited determinants and has been found to fix this problem. Based on our results we suggest to optimize the additional amplitudes $\tilde{t}_a^i$ independently from the conventional cluster amplitudes t_a^i in order to avoid undesired coupling between F12 corrections and one-electron contributions which has been found to cause a small but slowly diminishing bias in many cases. Using this XSP_{opt} ansatz, effectively converged correlation contributions can already be achieved using augmented QZ Dunning basis sets already, while even TZ basis sets typically yield satisfactory results. We have shown that terms containing $f(r_{12})$ aside from those included in the special F12 intermediates may be safely omitted without detrimental impact on the accuracy, leading to simplified and much more computationally efficient methods.

Whenever the one-electron basis set error impairs the total convergence, inclusion of the $T_{1'}$ operator typically leads to a considerable correction and may be used to improve the results, especially when small DZ and TZ basis sets are employed. However, this does not work equally well in all cases, indicating that the truncation criterion applied to the Lagrangian with respect to $T_{1'}$ is not yet ideal. Overall, the $\text{XSP}'_{\text{opt}}+T_{1'}$ ansatz has been demonstrated to provide highly reliable coupled-cluster methods which are well suited for the accurate calculation of static and dynamic response properties.

ACKNOWLEDGMENTS

This work has been funded by the Deutsche Forschungsgemeinschaft (Grant No. KO 2773/2). The authors also thank Jürgen Gauss for support.

[1] H. J. Monkhorst, Int. J. Quantum Chem. **S11**, 421 (1977).
[2] O. Christiansen, P. Jørgensen, and C. Hättig, Int. J. Quantum Chem. **68**, 1 (1998).
[3] R. J. Bartlett and M. Musiał, Rev. Mod. Phys. **79**, 291 (2007).
[4] E. A. Hylleraas, Z. Phys. **54**, 347 (1929).
[5] W. Kutzelnigg, Theor. Chim. Acta **68**, 445 (1985).
[6] J. Noga, W. Kutzelnigg, and W. Klopper, Chem. Phys. Lett. **199**, 497 (1992).
[7] H.-J. Werner, T. B. Adler, and F. R. Manby, J. Chem. Phys. **126**, 164102 (2007).
[8] W. Klopper, F. R. Manby, S. Ten-no, and E. F. Valeev, Int. Rev. Phys. Chem. **25**, 427 (2006).
[9] C. Neiss and C. Hättig, J. Chem. Phys. **126**, 154101 (2007).
[10] J. Yang and C. Hättig, J. Chem. Phys. **130**, 124101 (2009).
[11] H. Fliegl, C. Hättig, and W. Klopper, J. Chem. Phys. **124**, 044112 (2006).
[12] C. Neiss, C. Hättig, and W. Klopper, J. Chem. Phys. **125**, 064111 (2006).
[13] A. Köhn, J. Chem. Phys. **130**, 104104 (2009).
[14] S. Ten-no, Chem. Phys. Lett. **398**, 56 (2004).
[15] D. P. Tew and W. Klopper, J. Chem. Phys. **123**, 074101 (2005).
[16] S. Ten-no, J. Chem. Phys. **121**, 117 (2004).
[17] R. T. Pack and W. Byers Brown, J. Chem. Phys. **45**, 556 (1966).
[18] T. B. Adler, G. Knizia, and H.-J. Werner, J. Chem. Phys. **127**, 221106 (2007).
[19] G. Knizia, T. B. Adler, and H.-J. Werner, J. Chem. Phys. **130**, 054104 (2009).
[20] D. Bokhan, S. Ten-no, and J. Noga, Phys. Chem. Chem. Phys. **10**, 3320 (2008).
[21] A. Köhn, J. Chem. Phys. **130**, 131101 (2009).
[22] H. Fliegl, W. Klopper, and C. Hättig, J. Chem. Phys. **122**, 084107 (2005).
[23] D. P. Tew, W. Klopper, C. Neiss, and C. Hättig, Phys. Chem. Chem. Phys. **9**, 1921 (2007).
[24] D. P. Tew, W. Klopper, and C. Hättig, Chem. Phys. Lett. **452**, 326 (2008).
[25] A. Köhn, G. W. Richings, and D. P. Tew, J. Chem. Phys. **129**, 201103 (2008).
[26] T. Shiozaki, M. Kamiya, S. Hirata, and E. F. Valeev, J. Chem. Phys. **129**, 071101 (2008).
[27] The introduced intermediates $\mathcal{B}_{\text{I}}^X$ and $\mathcal{B}_{\text{II}}^X$ are analogous to the intermediates *A* and *Z* from Ref. 7.
[28] J. Noga and W. Kutzelnigg, J. Chem. Phys. **101**, 7738 (1994).
[29] DALTON, a molecular electronic structure program, Release 2.0, 2005, see http://www.kjemi.uio.no/software/dalton/dalton.html.
[30] E. F. Valeev, Chem. Phys. Lett. **395**, 190 (2004).
[31] See EPAPS supplementary material at http://dx.doi.org/10.1063/1.3238237 for data of response properties of BH, including a comparison of two formulations of $\mathcal{B}^X$ based on the auxiliary basis set convergence of α.
[32] M. Pecul, F. Pawłowski, P. Jørgensen, A. Köhn, and C. Hättig, J. Chem. Phys. **124**, 114101 (2006).
[33] D. P. Shelton and J. E. Rice, Chem. Rev. (Washington, D.C.) **94**, 3 (1994).
[34] K. Ruud and T. Helgaker, Chem. Phys. Lett. **352**, 533 (2002).
[35] T. Pedersen, H. Koch, L. Boman, and A. M. J. Sánchez de Merás, Chem. Phys. Lett. **393**, 319 (2004).
[36] T. D. Crawford, M. C. Tam, and M. L. Abrams, J. Phys. Chem. A **111**, 12057 (2007).
[37] P. Polavarapu, D. Chakraborty, and K. Ruud, Chem. Phys. Lett. **319**, 595 (2000).
[38] T. H. Dunning, Jr., J. Chem. Phys. **90**, 1007 (1989).
[39] D. E. Woon and T. H. Dunning, Jr., J. Chem. Phys. **100**, 2975 (1994).
[40] W. Klopper and C. C. M. Samson, J. Chem. Phys. **116**, 6397 (2002).
[41] F. Pawłowski, P. Jørgensen, and C. Hättig, Chem. Phys. Lett. **413**, 272 (2005).